RSC Advances

PAPER

View Article Online
View Journal | View Issue

Cite this: *RSC Adv.*, 2023, **13**, 2458

Experimental evidence for CH···π interaction-mediated stabilization of the square form in phenylglycine-incorporated ascidiacyclamide†

Akiko Asano, * Katsuhiko Minoura, Takeshi Yamada and Mitsunobu Doi

Ascidiacyclamide [cyclo(-Ile-oxazoline-D-Val-thiazole-)$_2$] is a cytotoxic cyclic peptide from ascidian. We examined the potential of the CH···π interaction at the diagonal position of ascidiacyclamide by comparing the interactions of Ile, Val, Abu (2-aminobutyric acid) or Ala with Ile, Chg (cyclohexylglycine) or Phg (phenylglycine). In solution, ascidiacyclamides are in a conformational equilibrium between square and folded forms. The CH···π interaction is expected to contribute to stabilization of the square form, which enhances the peptides' cytotoxicity. The distances between the alkyl side chain of Xaa and the π-plane of Phg were estimated from the crystal structures. The conformational free energies (Δ*G*°) determined through NMR-based quantitation indicated remarkable stabilization of the square form upon incorporation of Phg. These observations were consistent with the circular dichroism (CD) spectral measurements. Chemical shift perturbation studies suggested that stabilization of the square form of Phg-incorporated peptides was due to the CH···π interaction with the alkyl side chain of Xaa. Greater enthalpic losses were caused during the folding process of Phg-incorporated peptides than Ile- or Chg-incorporated peptides. It is suggested that these enthalpic losses are relevant to the CH···π interaction energies, which must be disrupted during folding. In addition, the CH···π interactions in the Phg-incorporated peptides increased cytotoxicity.

Received 7th November 2022
Accepted 4th January 2023

DOI: 10.1039/d2ra07063d

rsc.li/rsc-advances

Introduction

Ascidiacycalmide (**1a**) is a cytotoxic cyclic peptide isolated from the marine invertebrate ascidian.[1] The chemical sequence of **1a**, cyclo(-Ile^1-Oxz^2-D-Val^3-Thz^4-Ile^5-Oxz^6-D-Val^7-Thz^8-), contains the five-membered heterocycles oxazoline (Oxz) and thiazole (Thz) and is characterized by C_2-symmetry (Fig. 1). Previous structural analyses showed that **1a** assumes two major conformations, a "square form", which is the potentially cytotoxic structure, and a "folded form", and that the two conformations are in equilibrium in solution (Fig. 2).[2–9] The conformational free energies (Δ*G*°) of peptides bearing various substituents at the 1-position (or 5-position) were determined in NMR-based quantitative studies.[8] The ΔG°_{298K} value for a peptide bearing an *n*-propyl group was nearly zero, while those for peptides bearing a substituent smaller than an *n*-propyl group (**3a** and **4a**) were negative. On the other hand, the values for peptides bearing a bulkier substituent than an *n*-propyl group (**1a**, **2a**, **1b** and **1c**) were positive, which means that these peptides do not spontaneously fold at 298 K. This suggests that when **1a** is in the square form, the bulky side chain of the substituted amino acid residue and the *sec*-butyl group of the Ile residue at the diagonal position are close to each other, and the dispersion force between these two functional groups prevents spontaneous folding. In particular, a dispersion force like a CH···π interaction may be acting in peptides bearing a phenyl group (**1c**). While it is apparent that the van der Waals space occupied by a cyclohexyl group is larger than that of a planar phenyl group, the $\Delta G^{\circ}_{298\,K}$ value of **1c** is three times that of **1b**.

Phenylglycine (Phg) is a non-proteinogenic amino acid that is, nonetheless, a reported constituent of various natural peptidic products.[10–15] Phg can be regarded as a truncated version of Phe that lacks the methylene group. In other words, Phg has a bulky aromatic side chain directly attached to the α-carbon. It is therefore assumed that the degree of freedom of the aromatic ring side chain of Phg is strongly restricted, and the backbone conformation of a Phg-containing peptide is constrained accordingly. Furthermore, the electronic effects of aromatic moieties produce a weak noncovalent interaction, termed CH···π, which can contribute significantly to the proper folding and function of a protein.[16–22] For instance,

Faculty of Pharmacy, Osaka Medical and Pharmaceutical University, 4-20-1 Nasahara, Takatsuki, Osaka 569-1094, Japan. E-mail: akiko.asano@ompu.ac.jp; Fax: +81-72-690-1005; Tel: +81-72-690-1066

† Electronic supplementary information (ESI) available. CCDC 2191404 and 2191405. For ESI and crystallographic data in CIF or other electronic format see DOI: https://doi.org/10.1039/d2ra07063d

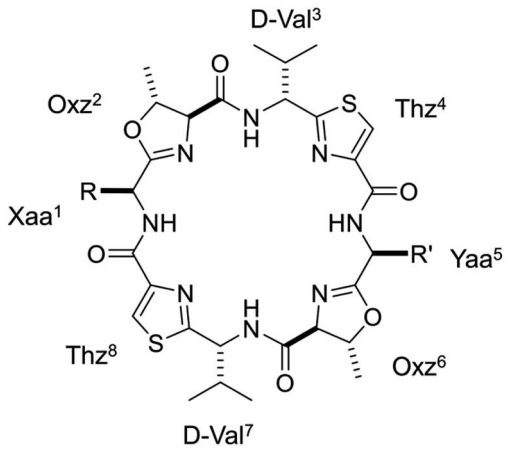

Position 1 \ Position 5	R' (Yaa5) (Ile5)	(Chg5)	(Phg5)
R (Xaa1) (Ile1)	**1a**2 Ascidiacyclaide	**1b**8	**1c**7
(Val1)	**2a**5	**2b**	**2c**
(Abu1)	**3a**8	**3b**	**3c**
(Ala1)	**4a**5	**4b**	**4c**

Fig. 1 Chemical structures of ascidiacyclamide and the side chains (R) of the Xaa[1] residues and the side chains (R′) of Yaa[5] residues. Peptides **1a**–**4a**, **1b** and **1c** were previously synthesized.[2,5,7,8] Peptides ***X*b** ($X = 2$–4) and ***X*c** ($X = 2$–4) are newly synthesized asymmetric analogues.

many saccharide units possessing codirected CH groups can bind into π clouds of aromatic moieties in proteins. Thus, the β-D-galactose bound to lectin makes contact with Phe131,[23] and the β-D-glucose bound to an *E. coli* chemoreceptor protein makes contact with Trp183.[24] The contact distances for these interactions were all within 3.5 Å within the X-ray structures. Given these steric and electronic features, it is expected that Phg would be a valuable pharmaceutical building block.

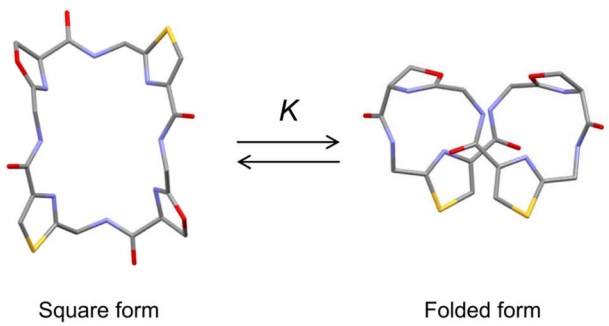

Fig. 2 Conformational equilibrium between the square and folded forms of ascidiacyclamide backbone. Carbon, nitrogen, oxygen and sulfur atoms are represented in gray, blue, red and yellow, respectively.

To gain additional details into the role of Phg in modulating the stability of square form, we investigated three series of peptides (***X*a**, ***X*b** and ***X*c**) in the present study (Fig. 1). The 5-position residues of ***X*a**, ***X*b** and ***X*c** peptides were Ile[5], cyclohexylglycine (Chg[5]) and Phg[5], respectively, and the 1-position residues were replaced with amino acid residues with substituents of various bulkiness [Ile ($X = 1$), Val ($X = 2$), 2-aminobutyric acid (Abu) ($X = 3$) and Ala ($X = 4$)]. Peptides **1a**–**4a**, **1b** and **1c** were previously synthesized, while peptides **2b**–**4b**, **2c**, **3c** and **4c** were newly synthesized. Here we describe their structural characterization based on X-ray diffraction, circular dichroism (CD) spectroscopy and variable temperature (VT) ^{1}H NMR measurements. We then discuss the impact of Phg on stabilization of the square form, which is the potentially cytotoxic structure, by making comparisons among the ***X*a**, ***X*b** and ***X*c** peptides.

Results and discussion

Crystal structures

The X-ray structures of **2b** and **2c** are shown in Fig. 3. For both **2b** and **2c**, each asymmetric unit contained the peptide molecule and one *N*,*N*-dimethylacetamide (DMA) molecule. Each peptide backbone was open, and the DMA molecule was located at the center of the peptide backbone, where it formed two hydrogen bonds with the peptide: N(D-Val[3])–H···O(DMA) and N(D-Val[7])–H···O(DMA) (Table 1). The previously reported crystal structure of **2a** was also a square form,[5] and there was no significant difference in the crystal structures among **2a**, **2b** and **2c**, whose 1-position is a Val residue. The crystal structures of **1a**, **1b** and **1c**, whose 1-position is an Ile residue, were also open.[2,7,8] On the other hand, the crystal structure of **4a** was folded.[5] In the ***X*a** peptides, the crystal structures were folded when the Xaa[1] residue side chain was small. However, the crystal structures of **3a**, **3b**, **3c**, **4b** and **4c** have not yet been determined.

The distances between the side chains of Xaa[1] and Phg[5] were estimated by surveying the CH···π contacts for the six-membered π-system, as described by Umezawa *et al.*[25–27] The distances from the H atoms of the Xaa[1] alkyl side chain to the π-orbital of the Phg[5] residue in the crystal structures of **1c** (ref. 7) and **2c** are shown in Fig. 4. The γ^1H of Ile[1] and the γ^2H of Val[1] were oriented in the direction opposite to the π-plane of Phg[5], and CH···π contacts were not observed. Within the crystal structure of **1c**, the δH of Ile[1] was located above the π-plane, but 4.52 Å away. The CH/π distance of the βH was 3.71 Å, while that of the γ^2H was 3.17 Å, which was the closest to the π-orbital. Within the crystal structure of **2c**, the CH/π distances of the βH and γ^1H of Val[1] were 4.00 Å and 3.75 Å, respectively. The sum of the van der Waals radii of the H and C_{sp^2} was 2.90 Å (1.20 Å for C–H plus 1.70 Å for a half

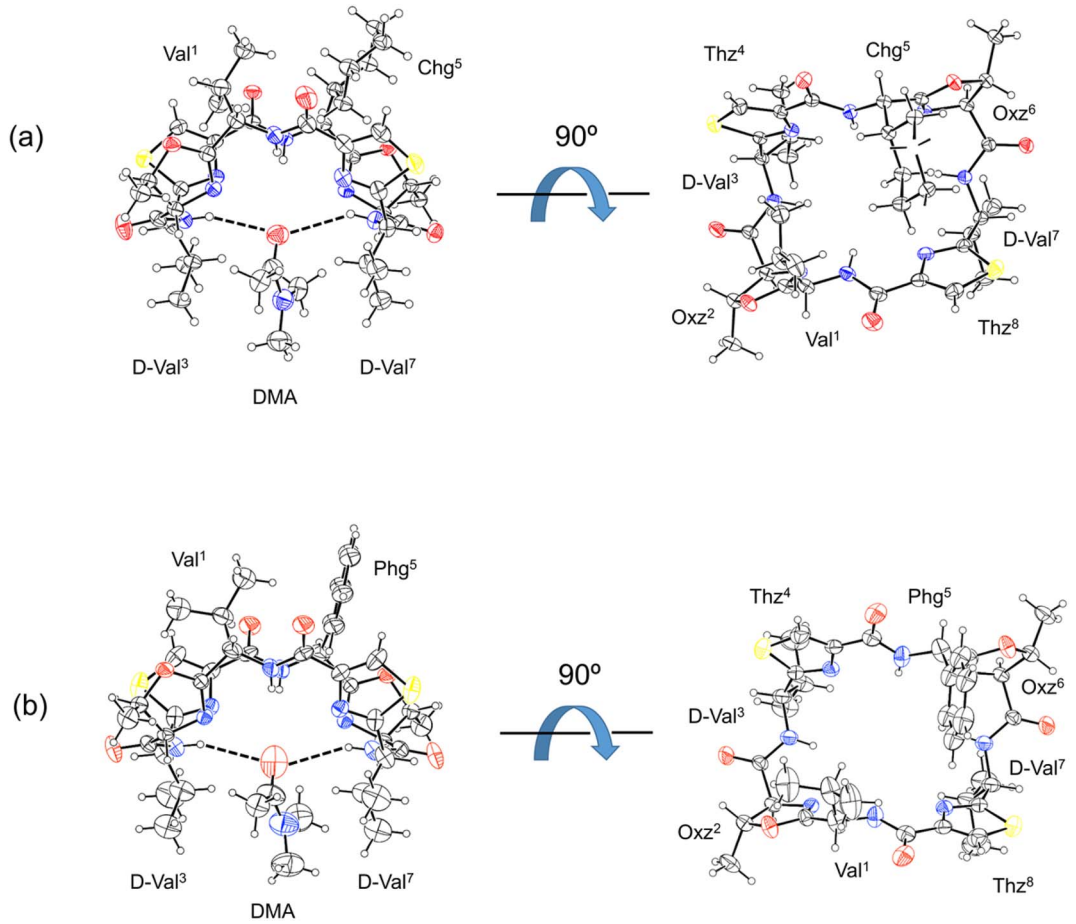

Fig. 3 Crystal structures of peptides **2b** and **2c** are presented in (a) and (b), respectively. Shown are the side (left) and top (right) views of the peptide rings. The dashed lines represent hydrogen bonds.

thickness of the aromatic molecule[28,29]), and more than 77% of organic crystals have been found to have CH/π distances shorter than 3.05 Å in database studies.[25–27] Although the CH/π distance between the γ^2H of Ile^1 and the π-orbital of Phg^5 in the crystal structure of **1c** was slightly longer than 3.05 Å, this distance makes it worth considering the presence of CH···π interactions.

CD spectra

The conformational equilibrium between the square and folded forms can be measured based on the CD spectral changes that occur while titrating 2,2,2-trifluoroethanol (TFE) into acetonitrile (CH_3CN) solution of the peptide.[5–9] For instance, the spectrum of **1a** in CH_3CN solution shows a positive band at around 205 nm and a negative band at around 245 nm, which is indicative of the square form. TFE titration led to decreases in $[\theta]_{205}$ and increases in $[\theta]_{245}$, which indicate the conformation of the peptide was folding.[5] By contrast, the spectrum of **4a** in CH_3CN solution shows a moderate positive band in the range of 230–260 nm, which is characteristic of the folded form. In other words, the conformational equilibrium position of **4a** in CH_3CN solution is significantly shifted in the forward direction, and there is almost no CD spectral change with TFE titration.[5] The conformational equilibria for ***X*b** and ***X*c** (X = 2–4) were measured using the same protocol. Their spectral changes are shown in Fig. 5 along with the previously recorded spectra of **1a–4a**,[5,8] **1b**[8] and **1c**[7] for comparison.

When the spectral changes among ***X*a**, ***X*b** and ***X*c** bearing the same Xaa[1] were compared, very similar spectral changes were seen in ***X*a** and ***X*b**, but those in ***X*c** indicated a large difference from the others. The spectra of all ***X*c** peptides in CH_3CN solution showed clearer negative bands around 245 nm than those of the corresponding ***X*a** and ***X*b** peptides. In particular, the

Table 1 Hydrogen bonds within the crystal structures of **2b** and **2c**

	Donor	Acceptor	Distance (Å)	Angle (°)
Peptide	D–H	A	D···A	∠D–H···A
2b	N(D-Val^3)–H	O(DMA)	3.223	150.45
	N(D-Val^7)–H	O(DMA)	3.381	143.04
2c	N(D-Val^3)–H	O(DMA)	3.387	150.63
	N(D-Val^7)–H	O(DMA)	3.387	150.63

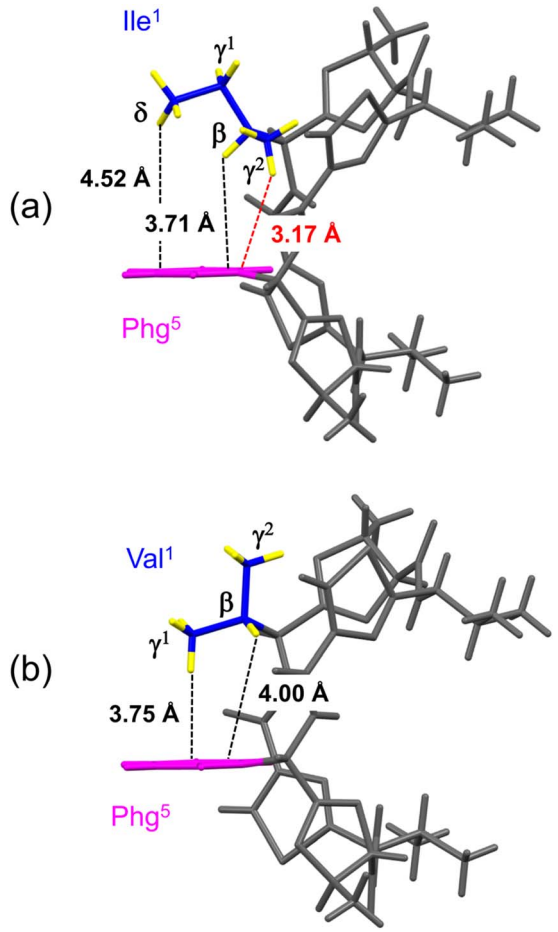

Fig. 4 Distances between the hydrogen atoms in the alkyl side chain of Xaa[1] and the π-orbital of Phg[5] within the crystal structures of **1c** (a) and **2c** (b). The alkyl carbon and hydrogen atoms of the Xaa[1] side chain and the aromatic moiety of the Phg[5] side chain are shown in blue, yellow and pink, respectively.

spectrum of **1c** in CH_3CN solution was not significantly affected by TFE, suggesting the conformational equilibrium position of **1c** is significantly shifted in the opposite direction. The incorporation of Chg[5] did not affect the conformational equilibrium, but incorporation of Phg[5] led to an apparent stabilization of the square form. For all ***X*a**, ***X*b** and ***X*c** peptides, folding became easier as the bulkiness of the Xaa[1] side chain declined (Ile[1] > Val[1] > Abu[1] > Ala[1]).

VT-^{1}H NMR

When the alkyl protons are close to the aromatic moiety, the result is a high-field shift of the alkyl proton chemical shift based on the ring-current effects of the aromatic ring. These high-field shifts can be probed to detect CH–π interactions.[30,31] The chemical shifts [δ (ppm)] for protons in the Xaa[1] alkyl side chain at 298 K and the chemical shift perturbations $\Delta\delta_{(Xb-X)}$ (ppm) and $\Delta\delta_{(Xc-Xa)}$ (ppm) are listed in Table 2. The values of $\Delta\delta_{(Xb-Xa)}$ and $\Delta\delta_{(Xc-Xa)}$ represent the magnitudes of the chemical shifts of alkyl protons in Xaa[1] caused by incorporation of Chg[5] and Phg[5], respectively. All absolute values of $\Delta\delta_{(Xb-Xa)}$ were very small, indicating that incorporation of Chg[5] had little effect on the chemical shift of the alkyl side chain of the Xaa[1] residue. By contrast, the high-field shifts of the alkyl side chain of the Xaa[1] residue caused by incorporation of Phg[5] were observed in all ***X*c** peptides and resulted in negative $\Delta\delta_{(Xc-Xa)}$ values for all Xaa[1] side chains in ***X*c** peptides. In addition, variable temperature ^{1}H NMR spectroscopy (VT-^{1}H NMR) was applied to examine the peptides every 10 K from 273 K to 333 K in CH_3CN-d_3 solution. The temperature coefficients [$\Delta\delta/\Delta T$ (ppb K^{-1})] for the alkyl protons in the Xaa[1] side chains that were high-field shifted by the ring-current effects of the π-orbital of the Phg[5] residue are shown in Fig. 6. In **1c**, the temperature coefficient for the γ^2H and βH in the Ile[1] residue were 2.1 and 1.7 ppb K^{-1}, respectively, which are significantly elevated values. Within the crystal structure of **1c**, the γ^2H was located closest to the π-plane of the Phg[5] residue, and the βH was second closest among the alkyl protons of the Ile[1] residue. These observations suggest that the high temperature coefficient for the γ^2H in the Ile[1] residue is due to a decrease in the CH···π interaction with increasing temperature. The temperature coefficient of the γH in the Abu[1] residue in **3c** also had a high temperature coefficient (2.0 ppb K^{-1}). Although the crystal structure of **3c** has not yet been determined, the position of the γH in the Abu[1] residue with respect to the π-plane of the Phg[5] residue may be similar to that of the γ^2H in the Ile[1] residue within the crystal structure of **1c**. Within the crystal structure of **2c**, one γH of the Val[1] residue was oriented toward the π-plane of the Phg[5] residue while the other γH was oriented toward the opposite side. However, the temperature coefficients of these two γ protons (1.2 and 1.4 ppb K^{-1}, respectively) did not significantly differ.

NMR-based quantification of the conformational equilibrium

The conformational equilibrium constants (K) of the peptides were determined based on the VT-H[1] NMR measurements. The thermodynamic parameters ($\Delta H°$, $\Delta S°$ and $\Delta G°$) were obtained from linear van't Hoff plots. These values are listed in Table 3. The $\Delta H°$ and $\Delta S°$ values for **1c** were not obtained because their K values exhibited no temperature dependency.[8] The folding of all peptides is enthalpically favorable ($\Delta H° < 0$) and entropically unfavorable ($\Delta S° < 0$). This thermodynamic profile results from four hydrogen bonds [N(Xaa[1])H···Oγ(Oxz[6]), N(D-Val[3])H···O(Thz[8]), N(Yaa[5])H···Oγ(Oxz[2]) and N(D-Val[7])H···O(Thz[4])] formed within the folded form. The ***X*a** and ***X*b** peptides have similar thermodynamic profiles, whereas the thermodynamic profiles of ***X*c** peptides differ from those of ***X*a** and ***X*b**. For ***X*c** peptides, the enthalpic terms were more unfavorable than those for either the ***X*a** or ***X*b** peptides. This suggests that the nature of the interactions between Xaa[1] and Ile[5] or Chg[5] are similar, but the interaction of Xaa[1] with Phg[5] is distinct. For the conformational change from the square to the folded form, it is necessary to through the transition state (TS) without the interaction between Xaa[1] and Yaa[5] (Fig. 7). It is considered that the folding of ***X*c** peptides causes an enthalpic loss

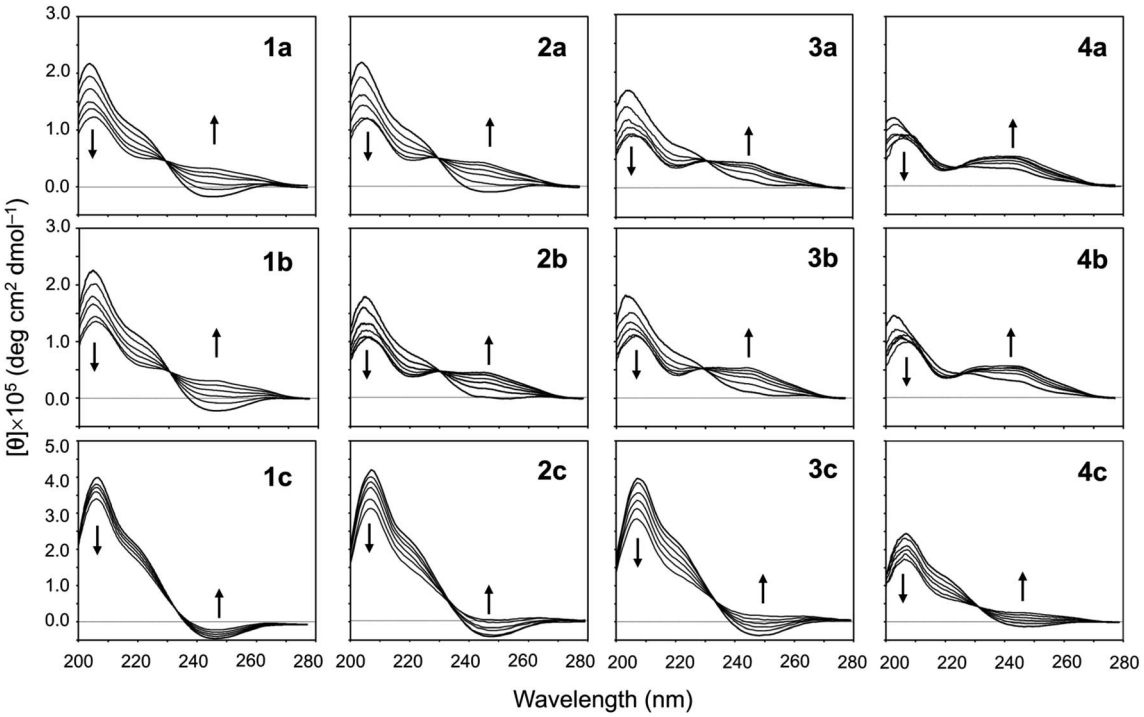

Fig. 5 CD spectral changes elicited by titration of TFE for peptides ***X*a**, ***X*b** and ***X*c** ($X = 1$–4). The CD spectra for ***X*a**, **1b** and **1c** were taken from previous reports.[5,7,8] The spectra were measured in CH_3CN solution while changing the TFE concentration (from 10% to 50% in increments of 10%).

$[\Delta\Delta H^\circ = \Delta H^\circ_{Xc} - \Delta H^\circ_{Xa}$ (or $\Delta H^\circ_{Xb})]$ by an amount related to the energy of the CH$\cdots\pi$ interaction.

Plots of the temperature *versus* ΔG° values for all peptides are shown in Fig. 8. The ΔG° values for **1a**, **1b** and all ***X*c** peptides were positive at every measured temperature. Comparing the results with the ***X*a** and ***X*b** peptides, the temperatures at which the ΔG° value of ***X*b** peptides was zero were about 5 K higher than those for the corresponding ***X*a** peptides (excluding **1a** and **1b**). This suggests that difficulty of spontaneous folding – *i.e.*, stability of the square form – among the peptides is in the order: ***X*c**, ***X*b**, ***X*a**. The ΔG° values at 298 K for all peptides are shown in Fig. 9. The ΔG°_{298K} value for ***X*a** peptides increases with increases in the bulkiness of the substituent of the Xaa[1] residue [methyl ($X = 4$) < ethyl ($X = 3$) < isopropyl ($X = 2$) < *sec*-butyl ($X = 1$)]. The same relationship between the bulkiness of the Xaa[1] side chain and the ΔG°_{298K} value was also seen with the ***X*b** and ***X*c** peptides. Among the ***X*a**, ***X*b** and ***X*c** peptides, the ΔG°_{298K} values of the ***X*c** peptides were clearly higher than those of the corresponding ***X*a** and ***X*b** peptides. These results suggest that in the square form of ***X*c**, the CH$\cdots\pi$ interaction was added to the dispersion force between the side chains of Xaa[1] and Yaa[5].

Cytotoxicity

The cytotoxicities of all the peptides were assessed by determining the ED_{50} against HL-60 human myeloblastic leukemia

Table 2 Chemical shifts (δ, ppm) for protons in the Xaa[1] alkyl side chain and chemical shift perturbations, $\Delta\delta_{(Xb-Xa)}$ (ppm) and $\Delta\delta_{(Xc-Xa)}$ (ppm), in CH_3CN-d_3 solution at 298 K

	Ile[1]				Val[1]			Abu[1]		Ala[1]
	βH	γ^1H	γ^2H	δH	βH	γH[a]	γH[a]	βH	γH	βH
***X*a**	1.91[b]	1.12[b], 1.23[b]	0.76[b]	0.68[b]	2.15[b]	0.85[b]	0.75[b]	1.95[c], 1.79[c]	0.78[c]	1.48[b]
***X*b**	1.94[c]	1.19[c], 1.35[c]	0.72[c]	0.76[c]	2.18	0.84	0.84	1.95, 1.82	0.73	1.44
***X*c**	1.45[d]	0.68[d], 0.98[d]	0.18[d]	0.37[d]	1.78	0.32	0.29	1.41, 1.41	−0.02	0.86
$\Delta\delta_{(Xb-Xa)}$	0.03	0.07, 0.12	−0.04	0.08	0.03	−0.01	0.09	0.00, 0.03	−0.05	−0.04
$\Delta\delta_{(Xc-Xa)}$	−0.46	−0.44, −0.25	−0.58	−0.31	−0.37	−0.53	−0.46	−0.54, −0.38	−0.83	−0.62

[a] The chemical shifts of two γ protons in the Val[1] residue are indistinguishable. [b] These data are taken from a previous report.[5] [c] These data are taken from a previous report.[8] [d] These data are taken from a previous report.[7]

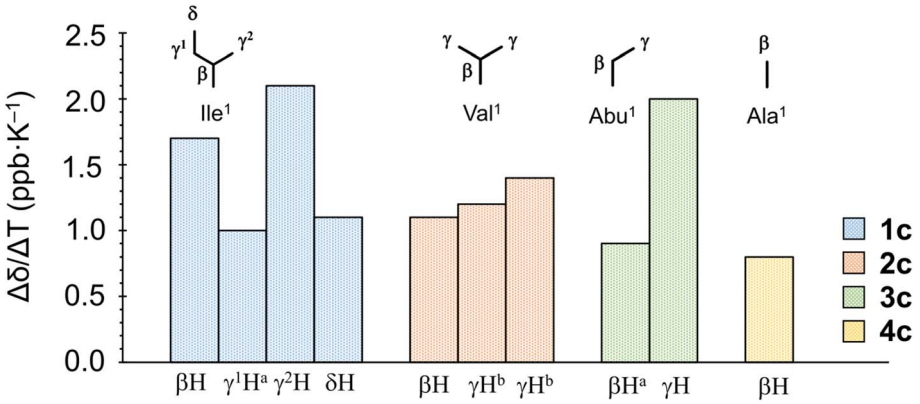

Fig. 6 Temperature coefficients [$\Delta\delta/\Delta T$ (ppb K^{-1})] of protons in the Xaa[1] alkyl side chain in the ***X*c** peptides. [a]Estimated from the average chemical shift of two protons of methylene. [b]The chemical shifts of the two γ protons in the Val[1] residue are indistinguishable.

cells, as described previously with some modification.[31,32] These results are listed in Table 4 along with previously obtained data for **1a** and **1c**. From the earlier results, it was concluded that the square form exhibits cytotoxicity and that the cytotoxicity is lessened by folding.[4–8] Among ***X*a** peptides, **3a** and **4a**, which have negative ΔG°_{298K} values, exhibited little or no cytotoxicity. Among ***X*b** peptides, **1b**, **3b** and **4b** exhibited stronger cytotoxicity than the corresponding ***X*a** peptides. The ΔG°_{298K} value of **1b** was equal to that of **1a**, but the cytotoxicity of **1b** was 7 times that of **1a**. Furthermore, despite having a negative ΔG°_{298K} value, **3b** and **4b** exhibited about 2–3 times stronger cytotoxicity than the parent peptide **1a**. Although the conformation and stability were very similar between the ***X*a** and ***X*b** peptides, there were significant differences in cytotoxicity. ***X*c** peptides, which assume the most stable square forms, exhibited stronger cytotoxicity than the corresponding ***X*a** peptides. However, the cytotoxicities of the ***X*b** peptides were equal to or greater than those of the ***X*c** peptides, except for **2b**.

Table 3 Thermodynamic parameters of peptides

Peptide	ΔH° (kJ mol^{-1})	ΔS° (J mol^{-1})	ΔG°_{298K} (kJ mol^{-1})
1a[a]	−9.55	−39.40	2.19
1b[a]	−9.85	−39.55	1.93
1c[a]	—[b]	—[b]	7.09
2a[a]	−13.01	−46.71	0.91
2b	−12.39	−43.16	0.47
2c	−5.38	−36.12	5.38
3a[a]	−13.83	−45.23	−0.35
3b	−11.78	−39.35	−0.06
3c	−5.79	−34.88	4.60
4a[a]	−16.76	−52.79	−1.03
4b	−15.72	−48.91	−1.15
4c	−10.58	−47.97	3.72

[a] Thermodynamic parameters of ***X*a** ($X = 1$–4), **1b** and **1c** are taken from a previous report.[8] [b] ΔH° and ΔS° values of **1c** were not obtained from the van't Hoff equation because their K values showed no temperature dependencies.

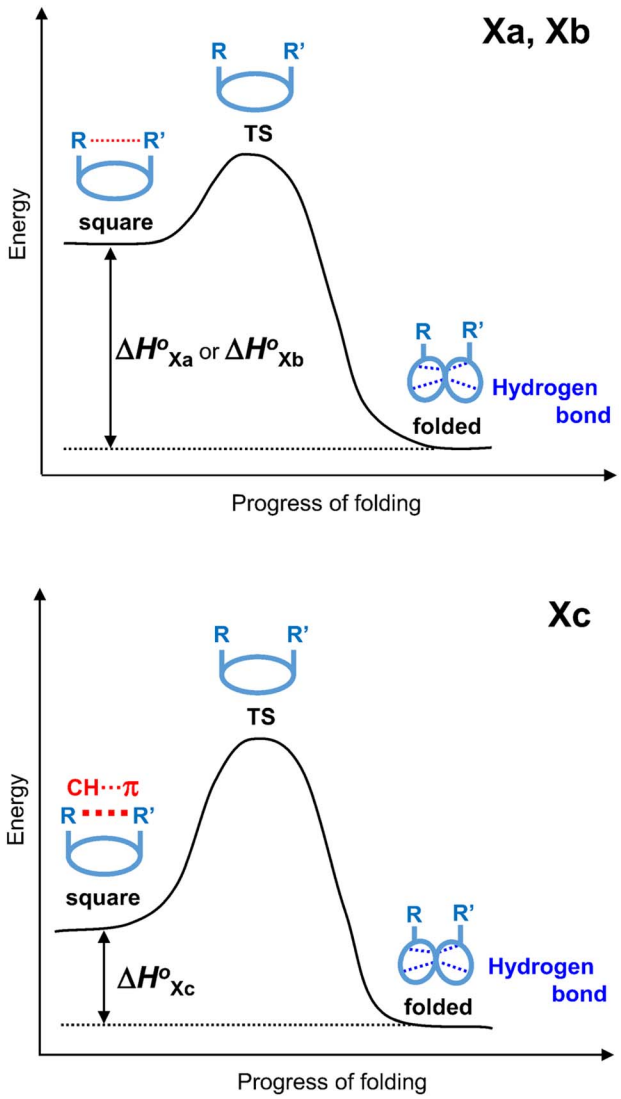

Fig. 7 Energy diagrams depicting the transition state (TS) between two conformers of ***X*a** and ***X*b** (top), and ***X*c** (bottom).

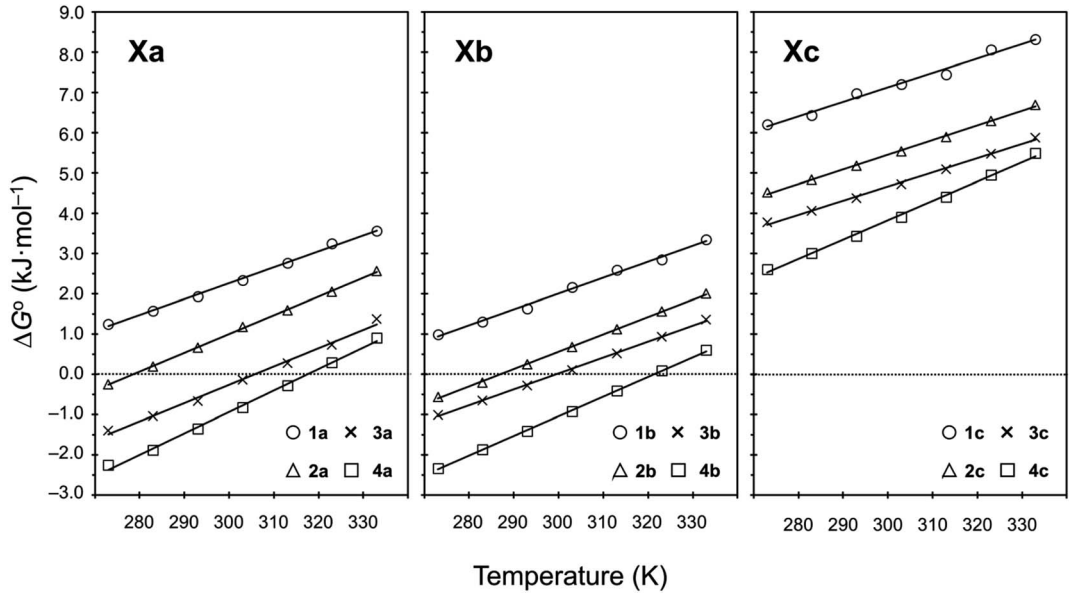

Fig. 8 Plots showing the temperature dependences of the free energies of the peptides. The data for *X***a** ($X = 1$–4), **1b** and **1c** were taken from a previous report.[8]

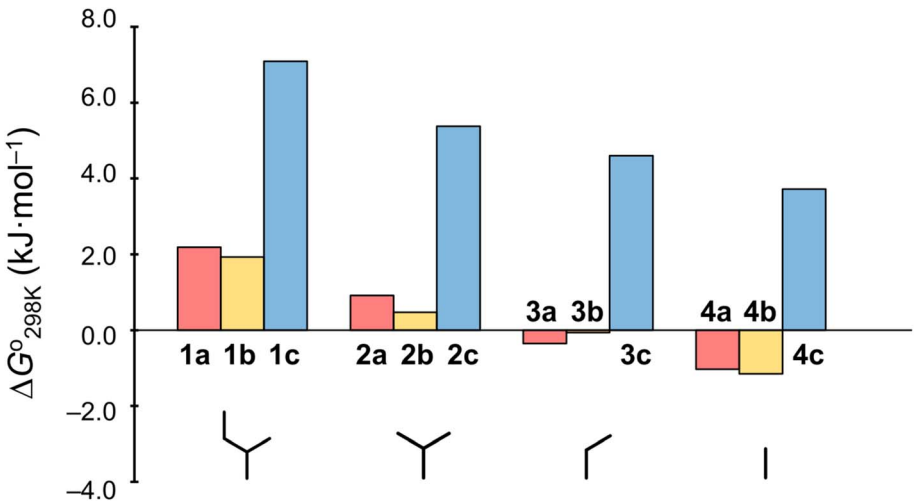

Fig. 9 Plots of the free energies of the peptides at 298 K. The ΔG°_{298K} values for *X***a**, *X***b** and *X***c** are represented by red, yellow and blue bars, respectively. The data for *X***a** ($X = 1$–4), **1b** and **1c** were taken from a previous report.[8]

Table 4 Cytotoxicities of peptides toward HL-60 cell

*X***a** peptides	ED_{50} (μg mL^{-1})	*X***b** peptides	ED_{50} (μg mL^{-1})	*X***c** peptides	ED_{50} (μg mL^{-1})
1a[a]	32.9 ± 0.9	**1b**	4.7 ± 0.03	**1c**[a]	12.7 ± 0.33
2a	21.1 ± 0.3	**2b**	35.3 ± 2.1	**2c**	4.6 ± 0.2
3a	>100	**3b**	10.7 ± 1.9	**3c**	12.2 ± 1.5
4a	54.9 ± 1.1	**4b**	19.0 ± 0.3	**4c**	16.5 ± 4.3

[a] These data are taken from a previous report.[7]

Conclusion

Our conformational studies carried out both in crystal and in solution, showed that incorporation of a Chg[5] residue does not affect the conformational equilibrium but incorporation of Phg[5] residue strongly promotes stabilization of the square form. It is considered that a CH···π interaction between the side chains of the Xaa[1] and Phg[5] residues is a key factor stabilizing the square form of ***X*c** peptides. The thermodynamic parameters estimated through NMR-based quantification provided strong evidences for this suggestion. The highly positive ΔG° values in the conformational equilibrium of ***X*c** peptides mean no spontaneous folding. The ΔH° values for the folding process of ***X*c** peptides were estimated to be 5–8 kJ mol^{-1} higher than those for the corresponding ***X*a** and ***X*b** peptides. These enthalpic losses are relevant to the CH···π interaction energies, which must be disrupted during the folding of ***X*c** peptides. Stabilization of the square form by the CH···π interaction also resulted in increased cytotoxicity.

Experimental

Peptide syntheses

The Thz unit (Boc-D-Val(Thz)-OMe) was synthesized as previously described.[32,33] The linear peptide Boc-Xaa-*allo*-Thr-D-Val-Thz-Yaa-*allo*-Thr-D-Val-Thz-OMe was synthesized using 1-hydroxybenzotriazole (Watanabe Chemical lnd. Ltd, Hiroshima, Japan) and 1-ethyl-3-(3-dimethylaminopropyl) carbodiimide hydrochloride (Watanabe Chemical lnd. Ltd, Hiroshima, Japan) in a liquid phase. Macrocyclization was accomplished using benzotriazolyloxy-tris(pyrrolidino)phosphonium hexafluorophosphate (Watanabe Chemical lnd. Ltd, Hiroshima, Japan) in the presence of 4-dimethylaminopyridine (Nacalai Tesque, Kyoto, Japan). The Oxz rings were formed by reacting the Xaa-*allo*-Thr and Yaa-*allo*-Thr moieties with bis(2-methoxyethyl)aminosulfur trifluoride (Deoxo-Fluor) (Fujifilm Wako Pure Chemical Corp., Osaka, Japan).[34] The synthesis and characterization of ***X*b** ($X = 2$–4) and ***X*c** ($X = 2$–4) are detailed in the ESI.†

X-ray diffraction

Peptides **2b** and **2c** were crystallized from *N*,*N*-dimethylacetamide (DMA). X-ray diffraction data for **2b** was collected with a Rigaku CrysAlis Pro (Rigaku Corp., Tokyo, Japan). X-ray diffraction data for **2c** was collected with a Bruker Smart APEXII (Bruker Corp., Massachusetts, USA). The structures of **2b** and **2c** were solved using SHELXS-97 (ref. 35) and refined using SHELXL-97.[35] The crystal data for both have been deposited with the Cambridge Crystallographic Data Center under deposition numbers 2191404 and 2191405, respectively. The crystal data for the two peptides are given in ESI.†

Circular dichroism

CD spectra were obtained using a JASCO spectra-polarimeter (model J-820, JASCO, Tokyo, Japan) with a 1 cm quartz cell at room temperature. The spectra were scanned in the range of 200–280 nm at a speed of 5 nm min^{-1} with a 0.1 nm interval for uptake to a computer. Data were averaged over each 1 nm and plotted. The spectra were measured in acetonitrile (CH_3CN) solution while changing the 2,2,2-trifluoroethanol (TFE) concentration (10%, 20%, 30%, 40% and 50%). Peptide concentrations were about 0.04 mM.

^{1}H NMR

^{1}H NMR spectra were recorded on an Agilent DD2 600 MHz NMR spectrometer (Agilent Technologies, California, USA). Peptide concentrations were about 5.0 mM in CH_3CN-d_3. Chemical shifts were measured relative to internal tetramethylsilane at 0.00 ppm. The protons were assigned using two-dimensional correlated spectroscopy (2D-COSY) and rotating-frame Overhauser effect spectroscopy (ROESY; mixing time = 500 ms). VT-^{1}H NMR measurements were made every 10 K from 273 K to 333 K. The assignment lists and 1D, 2D-COSY and ROESY spectra for ***X*b** ($X = 2$–4) and ***X*c** ($X = 2$–4) are given in ESI.†

NMR-based quantitative studies

The conformational equilibrium constants (K) (Fig. 2) of the peptides were determined as previously described.[8] The behaviors of the chemical shifts of conformationally sensitive Thz protons are the focus of this method. When the Thz rings face each other in the folded form, the chemical shifts for the Thz[4] and Thz[8] protons appear in a higher magnetic field than those in the square form due to the ring-current effects of the Thz[8] and Thz[4] rings, respectively. The K values of the peptides were estimated using eqn (1),

$$K = (\delta_S - \delta_{obs})/(\delta_{obs} - \delta_F) \quad (1)$$

where δ_{obs} is the chemical shift of the Thz protons in the equilibrating peptide, δ_S (=8.09 ppm) is the chemical shift of the Thz protons in T3ASC,[36] and δ_F (=7.35 ppm) is the chemical shift of the Thz protons in *d*ASC.[37] Two peptides, T3ASC and *d*ASC, were used as reference peptides to provide reference chemical shifts for the fully square and folded forms, respectively. The chemical structures of T3ASC and *d*ASC are given in ESI.†

The enthalpy (ΔH°) and entropy (ΔS°) were determined through a linear van't Hoff plot ($\ln K$ *versus* $1/T$), after which the Gibbs free energy (ΔG°) at 298 K was calculated using eqn (2).

$$\Delta G^\circ = \Delta H^\circ - T\Delta S^\circ = -RT \ln K \quad (2)$$

Assay for cytotoxicity

The cytotoxicity of the peptides was assessed using the 3-(4,5-dimethyl-2-thiazolyl)-2,5-diphenyl-2*H*-tetrazolium bromide (MTT) method as described previously with some modifications.[38,39] HL-60 human myeloblastic leukemia cells were cultured in RPMI 1640 medium (10% fetal calf serum) at 37 °C under 5% CO_2. The test materials were dissolved in dimethyl

sulfoxide to a concentration of 10 mM, after which that stock solution was diluted with essential medium to concentrations of 200, 20 and 2 μM. Each solution was combined with cells suspended (1×10^5 cells per mL) in the same medium. After incubating at 37 °C for 72 h under 5% CO_2, the cells were labeled with 5 mg mL^{-1} MTT in phosphate-buffered saline (PBS), and the absorbance of formazan dissolved in 20% sodium dodecyl sulfate in 0.1 N HCl was measured at 540 nm with a microplate reader (MTP-310, Corona electric Co. Ltd, Hitachinaka, Japan). The absorbance values are expressed as percentages relative to that of a control cell suspension prepared using the same procedure described above but without a test substance. All assays were performed three times, semilogarithmic plots were constructed from the averaged data, and the effective dose of a substance required to inhibit cell growth by 50% (ED_{50}) was determined.

Conflicts of interest

There are no conflicts to declare.

References

1 Y. Hamamoto, M. Endo, M. Nakagawa, T. Nakanishi and K. Mizukawa, *Chem. Commun.*, 1983, **6**, 323–324.
2 T. Ishida, M. Inoue, Y. Hamada, S. Kato and T. Shioiri, *Chem. Commun.*, 1987, **5**, 370–371.
3 T. Ishida, M. Tanaka, M. Nabae, M. Inoue, S. Kato, Y. Hamada and T. Shioiri, *J. Org. Chem.*, 1988, **53**, 107–112.
4 M. Doi, F. Shinozaki, Y. In, T. Ishida, D. Yamamoto, M. Kamigauchi, M. Sugiura, Y. Hamad, K. Kohda and T. Shioiri, *Biopolymers*, 1999, **49**, 459–469.
5 A. Asano, K. Minoura, T. Yamada, A. Numata, T. Ishida, Y. Katsuya, Y. Mezaki, M. Sasaki, T. Taniguchi, M. Nakai, H. Hasegawa, A. Terashima and M. Doi, *J. Pept. Res.*, 2002, **60**, 10–22.
6 A. Asano, T. Yamada, A. Numata and M. Doi, *Acta Crystallogr., Sect. A: Found. Crystallogr.*, 2003, **59**, o488–o490.
7 A. Asano, T. Yamada and M. Doi, *Bioorg. Med. Chem.*, 2011, **19**, 3372–3377.
8 A. Asano, K. Minoura, Y. Kojima, T. Yoshii, R. Ito, T. Yamada, T. Kato and M. Doi, *RSC Adv.*, 2020, **10**, 33317–33326.
9 A. Asano, M. Nakagawa, C. Miyajima, M. Yasui, K. Minoura, T. Yamada and M. Doi, *J. Pept. Sci.*, 2021, **27**, e3363.
10 C. Cocito, *Microbiol. Rev.*, 1979, **43**, 145–192.
11 J. C. Barriere, D. H. Bouanchaud, J. F. Desnottes and J. M. Paris, *Expert Opin. Invest. Drugs*, 1994, **3**, 115–131.
12 D. Vazquez, *J. Gen. Microbiol.*, 1966, **42**, 93–106.
13 Y. Mast and W. Wohlleben, *Int. J. Med. Microbiol.*, 2014, **304**, 44–50.
14 T. Teshima, M. Nishikawa, I. Kubota, T. Shiba, Y. Iwai and S. Omura, *Tetrahedron Lett.*, 1988, **29**, 1963–1966.
15 L. Brandi, S. Maffioli, S. Donadio, F. Quaglia, M. Sette, P. Milon, C. O. Gualerzi and A. Fabbretti, *FEBS Lett.*, 2012, **586**, 3373–3378.
16 M. Nishio, M. Hirota and Y. Umezawa, *The CH···π Interaction: Evidence, Nature and Consequences*, Wiley-VCH, New York, 1998.
17 E. A. Meyer, R. K. Castellano and F. Diederich, *Angew. Chem., Int. Ed.*, 2003, **42**, 1210–1250.
18 M. L. Waters, *Biopolymers*, 2004, **76**, 435–445.
19 C. D. Tatko and M. L. Waters, *J. Am. Chem. Soc.*, 2004, **126**, 2028–2034.
20 M. Harigai, M. Kataoka and Y. Imamoto, *J. Am. Chem. Soc.*, 2006, **128**, 10646–10647.
21 N. P. Brawell and A. P. Davis, *J. Org. Chem.*, 2011, **76**, 6548–6557.
22 C. J. Pace, D. Kim and J. Gao, *Chem. –Eur. J.*, 2012, **18**, 5832–5836.
23 N. K. Vyas, M. N. Vyas and F. A. Quiocho, *Science*, 1988, **242**, 1290–1295.
24 S. Elgavish and B. Shaana, *J. Mol. Biol.*, 1998, **277**, 917–932.
25 Y. Umezawa, S. Tsuboyama, K. Honda, J. Uzawa and M. Nishio, *Bull. Chem. Soc. Jpn.*, 1998, **71**, 1207–1213.
26 Y. Umezawa, S. Tsuboyama, H. Takahashi, J. Uzawa and M. Nishio, *Bioorg. Med. Chem.*, 1999, **7**, 2021–2026.
27 H. Suezawa, T. Yoshida, M. Hirota, H. Takahashi, Y. Umezawa, K. Honda, S. Tsuboyama and M. Nishio, *J. Chem. Soc., Perkin Trans. 1*, 2001, **2**, 2053–2058.
28 L. Pauling, *The Nature of the Chemical Bond*, Cornell University Press, Ithaca, New York, 1960, p. 260.
29 A. Bondi, *J. Phys. Chem.*, 1964, **68**, 441–451.
30 K. Kobayashi, Y. Asakawa, Y. Kikuchi, H. Toi and Y. Aoyama, *J. Am. Chem. Soc.*, 1993, **115**, 2648–2654.
31 I. Maeda, Y. Shimohigashi, I. Nakamura, H. Sakamoto, K. Kawano and M. Ohno, *Biochem. Biophys. Res. Commun.*, 1993, **193**, 428–433.
32 Y. Hamada, S. Kato and T. Shioiri, *Tetrahedron Lett.*, 1985, **26**, 3223–3226.
33 Y. Hamada, M. Shibata, T. Sugiura, S. Kato and T. Shioiri, *J. Org. Chem.*, 1987, **52**, 1252–1255.
34 A. J. Phillips, Y. Uto, P. Wipf, M. J. Reno and D. R. Williams, *Org. Lett.*, 2000, **2**, 1165–1168.
35 G. M. Sheldrick, *Acta Crystallogr., Sect. A: Found. Crystallogr.*, 2008, **64**, 112–122.
36 A. Asano, T. Yamada, T. Taniguchi, N. Sasaki, K. Yoza and M. Dio, *J. Pept. Sci.*, 2018, e3120.
37 A. Asano, M. Doi, K. Kobayashi, M. Arimoto, T. Ishida, Y. Katsuya, Y. Mezaki, H. Hasegawa, M. Nakai, M. Sasaki, T. Taniguchi and A. Terashima, *Biopolymers*, 2001, **58**, 295–304.
38 K. Kohda, Y. Ohta, Y. Yokoyama, T. Kato, Y. Suzumura, Y. Hamada and T. Shioiri, *Biochem. Pharmacol.*, 1989, **38**, 4497–4500.
39 K. Kohda, Y. Ohta, Y. Kawazoe, T. Kato, Y. Suzumura, Y. Hamada and T. Shioiri, *Biochem. Pharmacol.*, 1989, **38**, 4500–4502.